



HAL
open science

Synthesis, spectroscopic characterization, one and two-photon absorption properties, and electrochemistry of truxene π -expanded BODIPYs dyes

Jian Yang, Hao Jiang, Nicolas Desbois, Guoliang Zhu, Claude P. Gros,
Yuanyuan Fang, Frédéric Bolze, Shifa Wang, Hai-Jun Xu

► To cite this version:

Jian Yang, Hao Jiang, Nicolas Desbois, Guoliang Zhu, Claude P. Gros, et al.. Synthesis, spectroscopic characterization, one and two-photon absorption properties, and electrochemistry of truxene π -expanded BODIPYs dyes. *Dyes and Pigments*, 2020, 176, pp.108183-. 10.1016/j.dyepig.2020.108183 . hal-03489639

HAL Id: hal-03489639

<https://hal.science/hal-03489639>

Submitted on 21 Jul 2022

HAL is a multi-disciplinary open access archive for the deposit and dissemination of scientific research documents, whether they are published or not. The documents may come from teaching and research institutions in France or abroad, or from public or private research centers.

L'archive ouverte pluridisciplinaire **HAL**, est destinée au dépôt et à la diffusion de documents scientifiques de niveau recherche, publiés ou non, émanant des établissements d'enseignement et de recherche français ou étrangers, des laboratoires publics ou privés.



Distributed under a Creative Commons Attribution - NonCommercial 4.0 International License

Synthesis, spectroscopic characterization, one and two-photon absorption properties, and electrochemistry of truxene π -expanded BODIPYs dyes

Jian Yang,^{1,2} Hao Jiang,¹ Nicolas Desbois,² Guoliang Zhu,³ Claude P. Gros,^{2*}
Yuanyuan Fang,³ Frédéric Bolze,^{4*} Shifa Wang,¹ Hai-Jun Xu,^{1*}

¹ Jiangsu Co-Innovation Center of Efficient Processing and Utilization of Forest Resources, College of Chemical Engineering, Nanjing Forestry University, Nanjing 210037, China.

² ICMUB (UMR CNRS 6302), Université Bourgogne Franche-Comté, 21000 Dijon, France

³ Department of Chemistry and Chemical Engineering, Jiangsu University, Zhenjiang 212013, China

⁴ Conception et Applications des Molécules Bioactives (UMR CNRS - University of Strasbourg 7199) Faculté de Pharmacie, 74 route du Rhin, 67401 Illkirch (France)

Abstract

A series of mono- and bis-BODIPY substituted truxene derivatives were synthesized by the Knoevenagel condensation reaction and were fully characterized by NMR and HRMS. The photophysical properties of these new dyes have been investigated by UV-vis absorption spectroscopy, steady-state as well as time-resolved fluorescence spectroscopy and two-photon excited spectroscopy. Their electrochemical properties were investigated using cyclic voltammetry. The new dyes exhibit excellent photophysical properties in red to near-infrared region, including large extinction coefficients and high fluorescence quantum yields in methylene chloride solutions. These truxene-BODIPY dyads and triads also exhibit remarkable two-photon absorption cross section σ_2 up to 6000 GM at 800 nm.

Keywords: BODIPY, truxene, synthesis, photophysical properties, two-photon absorption, electrochemistry.

Introduction

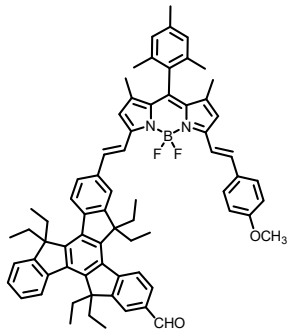
4,4-Difluoro-4-borato-3a,4a-diaza-s-indacene (BODIPY) is one of the most important fluorescent dyes and has received increasing attention in the last decade [1-3]. BODIPY dyes display excellent photophysical and optoelectronic properties, such as high photostability, large absorption coefficient in the visible and near-IR ranges, excellent chemical stability, high fluorescence quantum yields, a relatively long excited-state lifetime, good solubility in organic solvents, relative insensitivity to environmental conditions and good biocompatibility [3-5]. As a result, the BODIPY dyes are widely applied in Dye-Sensitized Solar Cells (DSSC) [6, 7], bioimaging [8, 9], photosynthetic-antenna reaction center mimics [10], photodynamic therapy [11], molecular switches [12], fluorescent probes/sensors [13], nonlinear optical materials [14], energy-transfer cassettes [15, 16], and molecular logic systems [17, 18]. In addition, the parent structure of the BODIPY dyes can easily be modified on all possible positions of the core, and functional groups can be introduced to the BODIPY for different applications [3, 19, 20]. In particular, BODIPY dyes also reveal remarkable two-photon absorption (TPA) by the introduction of electron donating (EDG) or withdrawing (EWG) groups [14, 21-23], though simple BODIPYs present low two-photon absorption cross sections. In recent years, the study of enhancing two-photon absorption performance by functional modification of the BODIPY structure has attracted considerable attentions [24, 25]. Therefore, the investigation of the photophysical properties of BODIPY derivatives is particularly interesting and greatly dependent on the functional groups [2, 3, 26]. In another hand, truxene is a C_3 -symmetric aromatic platform and plays an important role in constructing active materials as a promising building block in liquid crystals, supramolecular organizations and molecular energy donors [27, 28]. Moreover, the truxene unit can be also easily functionalized in three main directions at the C-2, C-7 and C-12 positions to serve as an excellent scaffold for the design of large star-shaped architectures [27-29]. Recently, many dyads, triads or other different chromophores based on truxene linking units have been synthesized and they have shown some potential applications in the area of solar cells [30-32], organic light-emitting diodes

(OLED) [33, 34], Non Linear Optical (including two-photon absorption) chromophores [24, 35-37], and organic fluorescent probes [38, 39]. For example, Donor-Acceptor truxene-bridged BODIPY triaryl zinc(II) porphyrin dyads were reported for energy transfer studies [40]. Also, truxene-BODIPY derivatives have shown to exhibit a reasonable two-photon absorption cross-section in the NIR region (700–900 nm) [24]. Particularly interesting, truxene core can efficiently enhance TPA activity, as was reported by Xiao *et al.* [41]. Therefore, in order to further investigate the cooperative effect of the truxene on the properties of the BODIPY derivatives, a series of dyads and triads truxene linking BODIPY *via* a C=C bond instead of previous C-C or C≡C linkers was designed (Chart 1). We report, in this work, the synthesis and spectroscopic characterization as well as absorption and emission spectroscopy and electrochemical properties of mono- and bis-substituted BODIPY truxene derivatives. Moreover, their two-photon absorption properties were also investigated.

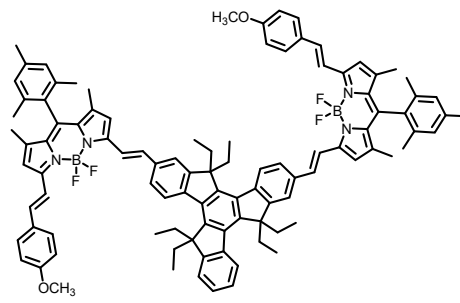
Results and discussion

Synthesis

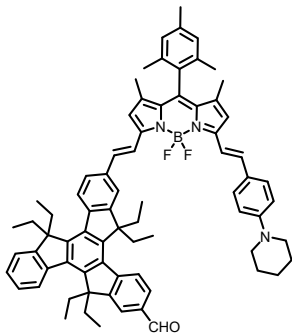
The structures of BODIPY derivatives **7a-d** and **8a-d** are shown in Chart 1. The synthetic route to access to **7a-d** and **8a-d** is depicted in Scheme 1. A very important linking block, 2,7-dicarboxaldehyde-5,5,10,10,15,15-hexaethyltruxene **2** was synthesized by treatment of 2,7-dibromo-5,5,1,10,15,15-hexaethyltruxene **1** with *n*-butyl lithium and DMF in dry diethyl ether solution. The BODIPY-truxene dyads **7a-d** and BODIPY-truxene-BODIPY triads **8a-d** were synthesized by a Knoevenagel condensation reaction between 2,7-dicarboxaldehyde **2** and different mono-styryl BODIPY derivatives **3-6** in the presence of *p*-toluenesulfonic acid and piperidine in dry toluene. All new compounds were fully characterized by ¹H NMR and HRMS which are shown in the ESI. NMR and HRMS analysis were consistent with the expected product structure.



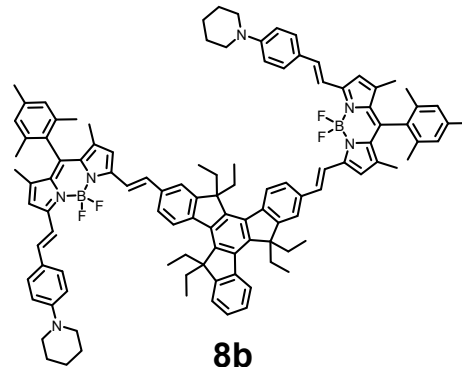
7a



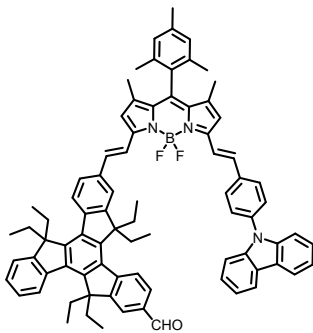
8a



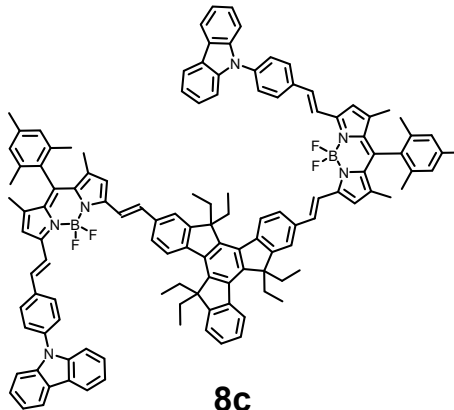
7b



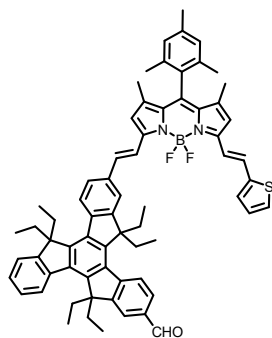
8b



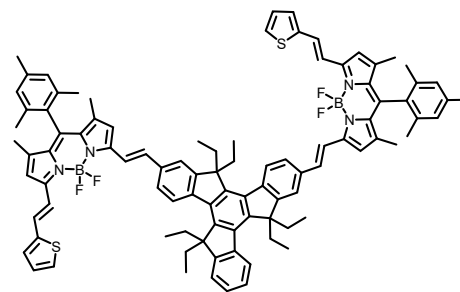
7c



8c

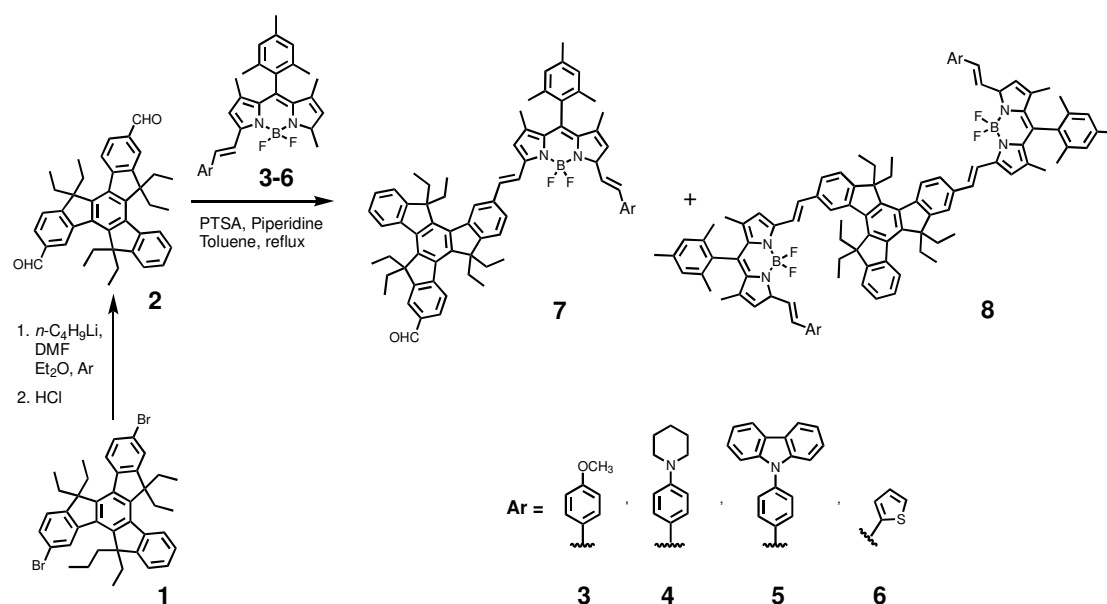


7d



8d

Chart 1



Scheme 1. Synthetic procedures and structures of dyes **7a-d** and **8a-d**.

One-photon photophysics

To gain further insight into their photophysical properties, the BODIPY dyads **7a-d** and triads **8a-d** were investigated by UV/Vis absorption as well as steady-state and time-resolved fluorescence spectroscopy in CH_2Cl_2 . The photophysical data are presented in Table 2. All compounds display absorption and emission spectra typical for BODIPY fluorophores. As shown in Figure 2, the absorption spectra of dyads **7a-d** exhibit a strong $S_0 \rightarrow S_1$ transition in the NIR region, which are located at 654 nm, 675 nm, 653 nm and 657 nm, for **7a**, **7b**, **7c** and **7d**, respectively. In comparison with the *meso*-mesityl substituted 1,3,5,7-tetramethyl BODIPY dye **1** [42], the maximum absorption peaks of **7a-d** shift bathochromically by 152 nm, 173 nm, 151 nm and 155 nm, respectively. Weaker and broader absorption bands centered at around 400 nm were observed at higher energy, which are attributed to $S_0 \rightarrow S_n$ ($n \geq 2$) transitions of the BODIPY moiety [43]. In addition, new bands at about 312 nm appear which could be ascribed to the truxene moiety ($S_0 \rightarrow S_1$ transition) [24]. In the case of truxene-bridged bis-BODIPY **8a-d**, their absorption spectra are almost unchanged compared with those of **7a-d** and their maximum absorption peaks appear at 659 nm, 677 nm, 659 nm and 662 nm, respectively, with only little bathochromic shifts of 2-6 nm in contrast to the corresponding dyads **7a-d**. This result indicates that the two BODIPY systems in the triads **8a-d** are not electronically coupled to each

other and almost lack of the effective π -conjugation. However, all compounds displayed high extinction coefficients in the range of 113000–325000 M⁻¹ cm⁻¹ (Table 2). Furthermore, the molar absorption coefficients of the triads **8a-d** are remarkably higher than those of the corresponding dyads **7a-d**.

The emission spectra of all the eight compounds were measured in CH₂Cl₂ solution. As shown in Figure 3, the emission peaks of these dyes are approximately the mirror image of their S₀ → S₁ absorption bands with small Stokes shift between 381 and 443 cm⁻¹ except for **7b** (1190 cm⁻¹) and **8b** (1202 cm⁻¹). For the dyads **7a-d**, the fluorescence emission maxima unambiguously appear in the NIR region and are centered at about 671 nm, 734 nm, 672 nm and 675 nm, respectively. Similar to the absorption, small redshifts of 3-7 nm in the emission bands are observed from **7a-d** to **8a-d**, which are located at 676 nm, 737 nm, 678 nm and 682 nm, respectively. However, the fluorescence quantum yields for triads **8a-d** (0.04-0.27) are much lower than those of the dyads **7a-d** (0.18-0.41, see Table 2). The triads **8a-d** bridging two BODIPY derivatives *via a* truxene moiety show lower fluorescence quantum yields possibly due to the intramolecular charge transfer (ICT) processes or the higher conformational flexibility induced by large molecular structure. In addition, the absorption and emission properties of these dyes are strongly influenced by the different substituents of the phenyl moieties. **7b** and **8b** bearing piperidinyl moieties exhibit remarkable bathochromic shifts in both absorption and emission spectra when compared to other dyads and triads, but much weaker fluorescence compared with **7a**, **7c-d** or **8a**, **8c-d** which are due to the strong intramolecular charge transfer driving from piperidinyl group. To further understand the fluorescence emission properties of **7a-d** and **8a-d**, the fluorescence lifetimes were determined to be 4.11 (**7a**), 3.94 (**8a**), 3.02 (**7b**), 3.07 (**8b**), 3.75 (**7c**), 3.64 (**8c**), 7.27 (**7d**) and 4.25 (**8d**) ns, respectively, which show a mono-exponential decay and consistent with their absorption and emission spectra.

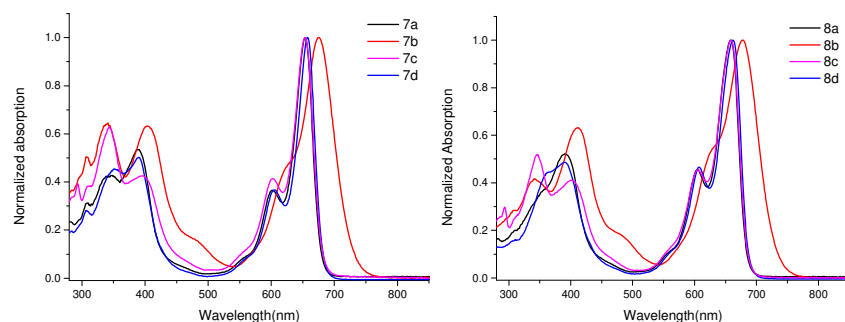


Figure 2. Normalized UV-vis absorption spectra of **7a-d** (left) and **8a-d** (right)

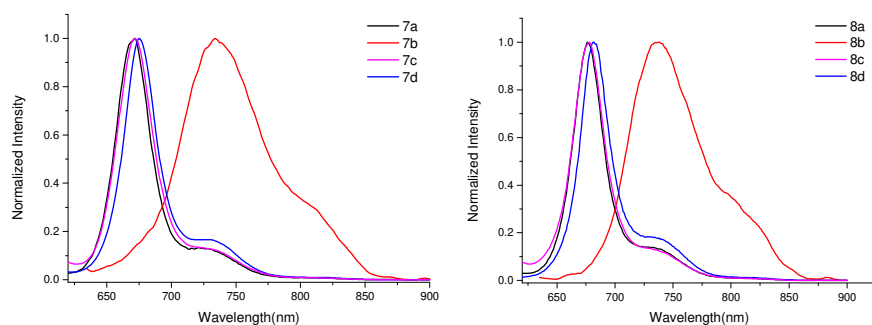


Figure 3. Normalized fluorescence spectra of **7a-d** (left) and **8a-d** (right)

Table 2. Photophysical properties of compounds **7a-d** and **8a-d** in DCM

Compound	$\lambda_{\text{abs}}[\text{nm}]$	$\lambda_{\text{em}}[\text{nm}]$	$\Delta\nu[\text{cm}^{-1}]$	$\epsilon[10^5 \cdot \text{M}^{-1} \cdot \text{cm}^{-1}]$	Φ_{F}	$\tau_{\text{F}}[\text{ns}]$
7a	654	671	387	1.98	0.41	4.11
8a	659	676	381	3.25	0.27	3.94
7b	675	734	1190	1.13	0.18	3.02
8b	677	737	1202	2.23	0.04	3.07
7c	653	672	433	1.57	0.37	3.75
8c	659	678	425	2.75	0.26	3.64
7d	657	675	406	1.51	0.40	4.27
8d	662	682	443	3.67	0.14	4.25

Two-photon absorption

Two-photon absorption properties of BODIPY-truxene derivatives **7a-d** and **8a-d** were investigated using the two-photon induced fluorescence method in the 750-1,000 nm range and two-photon excitation spectra **are shown** in Figure 4. The region studied corresponds to the $S_0 \rightarrow S_2$ transition. In contrast to the BODIPYs alone with various electron donating groups, the properties of this series of dyads and triads are very similar. All compounds exhibit two absorption maxima, one at about 800 nm and another one near 950 nm, corresponding to the two lower energy vibrational level of S_2 . The introduction of the truxene moiety in the chromophore induces a drastic

increase, up to a factor 10, in the TPA cross-sections, compared to the parent BODIPY alone. For example, the anisil substituted BODIPY has a σ_2 of 201 GM at 800 nm while the truxene dyad show a σ_2 of 2694 GM at the same wavelength. Surprisingly, no clear cooperative effect could be pointed out with the bis-BODIPY-truxene derivatives in the 800 nm zone, the bis-BODIPY TPA cross-section being the double of the mono-BODIPY. However, in the 950 nm zone, a cooperative effect can be pointed out, with an increase of a factor 3 in the σ_2 from the dyad to the triad for **7a**, **8a** and **8c**, and a factor 7 for the thiophene containing systems **7d** and **8d**. For the piperidine containing chromophore **7b** and **8b**, the values are surprisingly similar. Further theoretical investigations will be needed to explain this phenomenon. The two-photon absorption of the triads **8a-d** in the 800 nm range is of great importance regarding the future development of such type of fluorophore, with σ_2 over 5000 GM. Interestingly, the substitution on the BODIPY at the opposite side of the truxene branching induces much less effect than for the BODIPY alone as previously described in our preceding article [44].

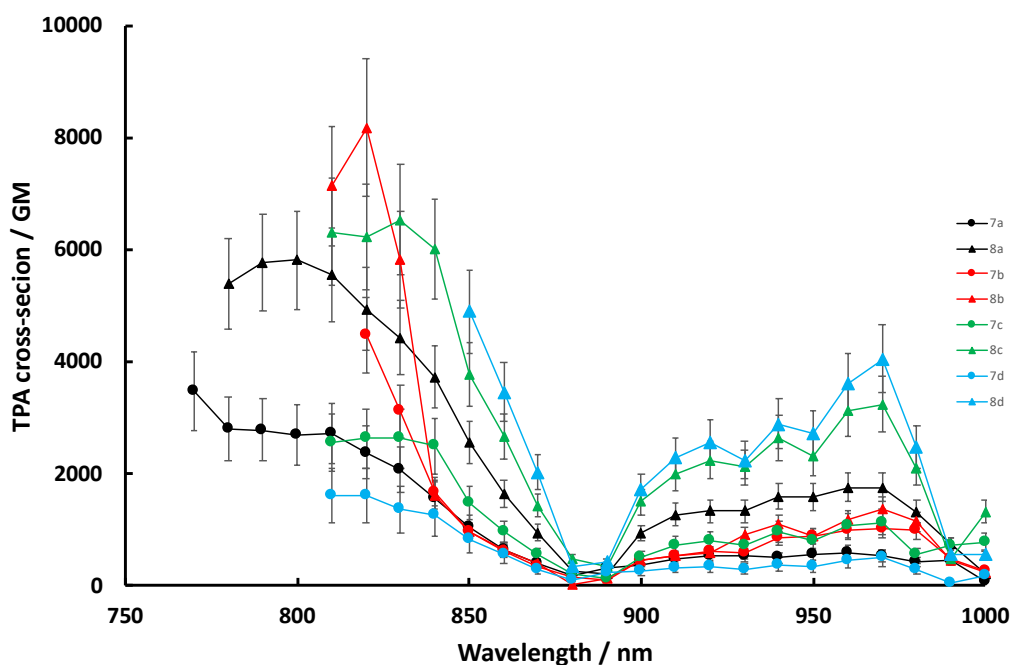


Figure 4. Two-photon excitation spectra of **7a-d** and **8a-d** in methylene chloride.

Electrochemistry

Redox properties of BODIPY derivatives **7a-d** and **8a-d** were investigated by cyclic voltammetry in dichloromethane with 0.1 M TBAP as supporting electrolyte at a scan rate of 0.1 V/s at room temperature. Measured redox potential for investigated compounds **7a-d** and **8a-d** were summarized in Table 3 and cyclic voltammograms of first reduction and first oxidation are shown in Figure 5. The first reduction and first oxidation potentials of the two series compounds are reversible and similar to each other. The first oxidation of **7a-d** located at $E_{1/2} = 0.79 \sim 0.87$ V) and first reduction at $E_{1/2} = -0.95 \sim -1.04$ V). Compounds **8a-d** shows similar redox potential as **7a-d** with first oxidation at 0.71 ~ 0.86 V and first reduction at -0.97~ -1.05 V. As compared to compounds **7a-d**, compounds **8a-d** have two overlapped one electron transfer each step on the two electroactive BODIPY rings. This overlapped electron transfer process further proved that there is a lack of effective π -conjugation between the two BODIPY moieties. It is worthy to remind that compounds **7b** and **8b** show an addition reversible oxidation at 0.57 and 0.56 V, maybe due to the oxidation of the linked functional group.

As compared to the parent BODIPY dye (first oxidation at $E_{1/2} = 1.21$ V and first reduction at $E_{1/2} = -1.24$ V) [42], both the first reduction and first oxidation of **7a-d** and **8a-d** were shifted to an easier direction and significantly decreased the HOMO-LUMO gap. This is because the vinyl substituents at 3,5-positions of the parent BODIPY increases electronic delocalization and causes remarkable stabilization of the LUMO and destabilization of the HOMO, which will narrow the HOMO-LUMO gap and hence result in the red shift of the lowest-energy absorption bands. In addition, it is clear that different substituents on the 3,5-position except for piperidyl group have slight influence on their electrochemical properties. These conclusions were further confirmed by comparison of the absorption and emission spectra of these dyad or triad dyes with the single BODIPY dyes.

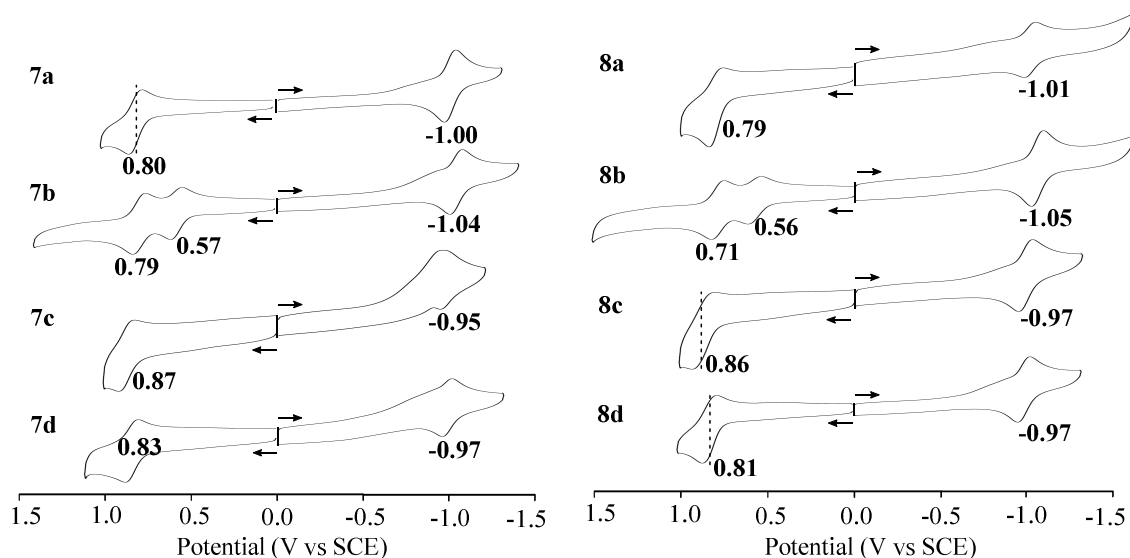


Figure 5. Cyclic voltammograms of compounds **7a-d** and **8a-d** in CH_2Cl_2 containing 0.1M TBAP at a scan rate of 0.1 V/s.

Table 3. Cyclic voltammetry of compounds **7a-d** and **8a-d** in CH_2Cl_2 containing 0.1M TBAP at a scan rate of 0.1 V/s.

Cpd	1 st Ox (V)	1 st Red (V)	H-L ^a (v)
7a	0.80	-1.00	1.80
7b	0.57	-1.04	1.61
7c	0.87	-0.95	1.82
7d	0.83	-0.97	1.80
8a	0.79	-1.01	1.80
8b	0.56	-1.05	1.61
8c	0.86	-0.97	1.83
8d	0.81	-0.97	1.78

^aThe potential difference between the first oxidation and first reduction (the HOMO–LUMO gap) measured on the CV voltammograms.

Conclusion

In conclusion, we have prepared and characterized a series of eight new BODIPY-truxene derivatives. The excellent TPA cross-sections combined to reasonable fluorescence quantum yield (the product of σ_2 by Φ being the two-photon brightness up to 1500 GM in the 800 nm range) in the tissue transparency window

make these fluorophores good candidates for application in bioimaging after *e.g.* water solubilization or incorporation in lipophilic nanoparticles.

Experimental Section

1.1. General

All chemicals and solvents were of analytical reagent grade and used directly as received unless otherwise noted. Solvents for reactions were purified and dried according to standard procedures, and then distilled before use. Dichloromethane (99.8%) was purchased from Sinopharm Chemical Reagent Co. and fresh distilled before use for electrochemistry. Tetra-*n*-butylammonium perchlorate (TBAP) from Sigma Chemical was recrystallized from ethyl alcohol, and dried under vacuum at 40 °C for at least one week before use. All mixtures of solvents are given in v/v ratio. ¹H NMR spectra were collected on a Bruker DRX-600 AVANCE III spectrometer. Chemical shifts for ¹H NMR spectra were recorded in ppm relative to CDCl₃ ($\delta = 7.26$ ppm) as the internal standard. Mass spectra data were obtained using a Thermo Fisher LTQ Orbitrap XL (HR-ESI) spectrometer.

1.2 Spectroscopic measurements.

UV-vis spectra were carried out on a Shimadzu UV-3100 spectrophotometer. All the Spectra and PLQY were measured in FluoroLog-UltraFast (HORIBA Instrument Inc, Edison) equipped with a 450 W CW xenon lamp and an Open-Electrode TECooled CCD Detector (Syncerity). Absorption and emission measurements were carried out in 1×1 cm quartz cuvettes with spectroscopic grade solvent, and was kept constant at (298 ± 2) K. An integrating sphere mounted in sample compartment directly for PLQY measure. Nanosecond lifetime and TRES studies were conducted using a TCSPC MCA model equipped with a picosecond photo detector (<200 ps) (PPD850) and picosecond laser (duration is 180 ps, Deltadiode, 100 MHz laser). TRES data were measured by incrementing the monochromator on the emission channel of the time-resolved fluorometer in fixed wavelength intervals at each wavelength. Slices of data were taken in the intensity-wavelength plane to obtain spectra at different times during the decay. Microsecond lifetime decays were collected by a MCS mode on

TCSPC HUB (DeltaHUB) with a LED source (SpectraLED) as a sample excitation source. The fluorescence lifetime values were obtained from deconvolution and distribution lifetime analysis.

1.3 Electrochemistry. Cyclic voltammetry was performed at 298 K on a CHI-730C Electrochemical Workstation. A homemade three-electrode cell was used for cyclic voltammetric measurements and composed of a glassy carbon working electrode, a platinum wire counter electrode and a homemade saturated calomel reference electrode (SCE). The SCE was separated from the bulk of the solution by a fritted glass bridge of low porosity which contained the solvent/supporting electrolyte mixture.

1.4 Two-photon spectroscopy

The TPA cross-section spectra were obtained by the fluorescence method as described previously [45]. Briefly, a Ti:sapphire femtosecond laser (Insight Spectra Physics) in the range 750-1,000 nm was used for excitation. The excitation beam is collimated over the cell length (10 mm). The fluorescence, collected at 90° of the excitation beam, was focused into an optical fiber connected to a spectrometer. The incident beam intensity was adjusted to ensure an intensity-squared dependence of the fluorescence over the whole spectral range. Calibration of the spectra was performed by comparison with Rhodamine B in MeOH [46, 47] and Fluorescein in 0.1N NaOH solution [46].

1.5 Synthesis

2,7-Dibromo-5,5,10,10,15,15-hexaethyltruxene **1** and compounds **3-6** were synthesized according to the reported literature [44, 48].

Synthesis of 2, 7-dicarboxaldehyde-5, 5, 10, 10, 15, 15-hexaethyltruxene **2**

A Schlenk flask was charged with 2,7-dibromo-5,5,10,10,15,15-hexaethyltruxene (5.00 mmol, 3.34 g) dissolved in dry diethyl ether (240 mL) under an argon atmosphere. The solution was cooled to -78 °C, then *n*-BuLi (30.0 mmol, 2.5 M, 12.0 mL) was added dropwise and stirred for 30 min. After removing the cold bath, the reaction was stirred for another 30 min at room temperature. The solution was again cooled to -78 °C, followed by dropwise addition of dry DMF (33.2 mmol, 2.50 mL), then the cold bath was removed and the reaction mixture was kept under stirring

overnight at room temperature. The reaction was then quenched by HCl (2 N, 200 mL), and stirred for 2 h. The mixture was washed with diethyl ether and water and dried over Na₂SO₄. The solvent was removed under reduced pressure. The crude product was further purified using column chromatography on silica gel to obtain 2,7-dicarboxaldehyde-5,5,10,10,15,15-hexaethyltruxene **2** (2.12 g, 75% yield). ¹H NMR (CDCl₃, 600 MHz, ppm) δ 10.14 (s, 2H), 8.51-8.55 (m, 2H), 8.36-8.38 (m, 1H), 8.01 (s, 2H), 7.94 (d, *J* = 7.8 Hz, 2H), 7.48-7.51 (m, 1H), 7.43-7.45 (m, 2H), 2.96-3.10 (m, 6H), 2.19-2.3 (m, 6H), 0.19-0.23 (m, 18H).

Synthesis of compounds **7a** and **8a**

In a 50 mL three-neck round bottom flask with a dean-stark apparatus, compound **3** (0.25 mmol, 120 mg), 2,7-dicarboxaldehyde-5,5,10,10,15,15-hexaethyltruxene (0.16 mmol, 93 mg), *p*-toluenesulfonic acid (0.4 mmol, 70 mg), dry toluene (25 mL) and piperidine (2 mL) were added. After heating to reflux, the progress of the reaction was monitored by TLC, the reaction was stopped until 2,7-dicarboxaldehyde-5,5,10,10,15,15-hexaethyltruxene disappeared completely. The mixture was cooled to room temperature, which was poured into brine (50 mL), extracted with dichloromethane (3 × 50 mL). The combined organic phase was dried over anhydrous sodium sulfate and the solvent was evaporated on a rotary evaporator under reduced pressure. The resulting crude residue was purified by silica gel column chromatography, eluted with CH₂Cl₂/petroleum ether = 1:1 (in vol.), giving **7a** (37 mg, 15% yield) and **8a** (23 mg, 6% yield). **7a**: ¹H-NMR (600 MHz, CDCl₃, ppm): δ 10.14 (s, 1H), 8.57-8.53 (m, 1H), 8.42-8.36 (m, 2H), 8.01 (d, *J* = 6.6 Hz, 1H), 7.94 (t, *J* = 7.8 Hz, 1H), 7.85 (d, *J* = 16.2 Hz, 1H), 7.78 (d, *J* = 7.8 Hz, 1H), 7.67 (d, *J* = 16.2 Hz, 1H), 7.63 (m, 3H), 7.51-7.48 (m, 1H), 7.45-7.38 (m, 3H), 7.28-7.25 (d, *J* = 16.2 Hz, 1H), 6.98 (d, *J* = 6.0 Hz, 4H), 6.70 (s, 1H), 6.64 (s, 1H), 3.89 (s, 3H), 3.11-2.95 (m, 6H), 2.36 (s, 3H), 2.31-2.19 (m, 6H), 2.15 (s, 6H), 1.48 (s, 3H), 1.47 (s, 3H), 0.26-0.23 (m, 18H). HRMS (ESI): [M]⁺, C₇₁H₇₁BF₂N₂O₂ calculated: 1032.5577; found: 1032.5625. **8a**: ¹H-NMR (600 MHz, CDCl₃, ppm): δ 8.44-8.40 (m, 3H), 7.86 (d, *J* = 16.2 Hz, 2H), 7.79 (d, *J* = 7.8 Hz, 2H), 7.69 (d, *J* = 16.2 Hz, 2H), 7.63 (d, *J* =

7.8 Hz, 6H), 7.50 (d, $J = 6.6$ Hz, 1H), 7.45-7.39 (m, 4H), 7.27-7.24 (d, $J = 15.6$ Hz, 2H), 6.99-6.96 (m, 8H), 6.70 (s, 2H), 6.64 (s, 2H), 3.83 (s, 6H), 3.11-3.01 (m, 6H), 2.37 (s, 6H), 2.31-2.19 (m, 6H), 2.16 (s, 12H), 1.49 (s, 6H), 1.48 (s, 6H), 0.30-0.25 (m, 18H). HRMS (ESI): $[M]^+$, $C_{101}H_{100}B_2F_4N_4O_2$ calculated: 1498.7969; found: 1498.8153.

Synthesis of compounds **7b** and **8b**

Compounds **7b** and **8b** were obtained by following a procedure similar to that of **7a** and **8a** as a deep red solid in 8% and 13% yield, respectively. Compound **7b**: 1H -NMR (600 MHz, $CDCl_3$, ppm): δ 10.14 (s, 1H), 8.58-8.53 (m, 1H), 8.42-8.36 (m, 2H), 8.02 (d, $J = 7.2$ Hz, 1H), 7.94 (t, $J = 16.2$ Hz, 1H), 7.87 (d, $J = 16.2$ Hz, 1H), 7.79-7.75 (m, 1H), 7.65-7.62 (m, 2H), 7.58 (d, $J = 8.4$ Hz, 2H), 7.51-7.48 (m, 1H), 7.45-7.36 (m, 3H), 7.28-7.25 (d, $J = 16.2$ Hz, 1H), 6.98 (s, 2H), 6.96 (d, $J = 7.2$ Hz, 2H), 6.69 (s, 1H), 6.65 (s, 1H), 3.33 (m, 4H), 3.11-2.96 (m, 6H), 2.36 (s, 3H), 2.32-2.19 (m, 6H), 2.15 (s, 6H), 1.75-1.72 (m, 4H), 1.67-1.63 (m, 2H), 1.48 (s, 3H), 1.47 (s, 3H), 0.27-0.20 (m, 18H). HRMS (ESI): $[M+H]^+$, $C_{75}H_{79}BF_2N_3O$ calculated: 1086.6284; found: 1086.6333. Compound **8b**: 1H -NMR (600 MHz, $CDCl_3$, ppm): δ 8.47-8.41 (m, 3H), 7.89 (d, $J = 16.2$ Hz, 2H), 7.81-7.77 (m, 2H), 7.68-7.63 (m, 4H), 7.59-7.58 (m, 4H), 7.50 (d, $J = 7.8$ Hz, 1H), 7.46-7.39 (m, 4H), 7.28-7.25 (d, $J = 16.2$ Hz, 2H), 6.99 (s, 4H), 6.96-6.93 (m, 4H), 6.71 (s, 2H), 6.66 (s, 2H), 3.30-3.27 (m, 8H), 3.14-3.03 (m, 6H), 2.37 (s, 6H), 2.34-2.20 (m, 6H), 2.17 (s, 12H), 1.71-1.67 (m, 8H), 1.63-1.59 (m, 4H), 1.50 (s, 6H), 1.48 (s, 6H), 0.32-0.26 (m, 18H). HRMS (ESI): $[M+H]^+$, $C_{109}H_{115}B_2F_4N_6$ calculated: 1605.9305; found: 1605.9462.

Synthesis of compounds **7c** and **8c**

Compounds **7c** and **8c** were obtained by following a procedure similar to that of **7a** and **8a** as a deep red solid in 15% and 13% yield, respectively. Compound **7c**: 1H -NMR (600 MHz, $CDCl_3$, ppm): δ 10.12 (s, 1H), 8.53-8.51 (m, 1H), 8.42-8.35 (m, 2H), 8.19-8.14 (m, 2H), 7.99-7.98 (m, 1H), 7.93-7.87 (m, 5H), 7.80 (d, $J = 7.8$ Hz, 1H), 7.67-7.65 (m, 2H), 7.62 (s, 1H), 7.53 (d, $J = 8.4$ Hz, 2H), 7.48-7.45 (m, 3H), 7.42-7.39 (m, 3H), 7.36-7.32 (m, 3H), 7.00 (s, 2H), 6.73 (s, 1H), 6.72 (s, 1H), 3.10-2.94 (m, 6H), 2.38 (s, 3H), 2.29-2.20 (m, 6H), 2.18 (s, 6H), 1.51 (s, 6H),

0.26-0.21 (m, 18H). HRMS (ESI): $[M]^+$, $C_{82}H_{76}BF_2N_3O$ calculated: 1167.6050; found: 1167.6169. Compound **8c**: 1H -NMR (600 MHz, $CDCl_3$, ppm): δ 8.40 (t, $J = 6.0$ Hz, 2H), 8.35 (d, $J = 7.2$ Hz, 1H), 8.17 (d, $J = 7.8$ Hz, 4H), 7.91-7.86 (m, 9H), 7.76 (d, $J = 7.2$ Hz, 1H), 7.62 (m, 5H), 7.55 (s, 1H), 7.52-7.50 (m, 4H), 7.46-7.42 (m, 7H), 7.38-7.37 (m, 3H), 7.34-7.31 (m, 6H), 7.01 (s, 4H), 6.74-6.72 (m, 4H), 3.08-2.98 (m, 6H), 2.39 (s, 6H), 2.25-2.15 (m, 18H), 1.52 (s, 12H), 0.27-0.20 (m, 18H). HRMS (ESI): $[M+H]^+$, $C_{123}H_{111}B_2F_4N_6$ calculated: 1769.8992; found: 1769.9153.

Synthesis of compounds **7d** and **8d**

Compounds **7d** and **8d** were obtained by following a procedure similar to that of **7a** and **8a** as a deep red solid in 13% and 5% yield, respectively. Compound **7d**: 1H -NMR (600 MHz, $CDCl_3$, ppm): δ 10.14 (s, 1H), 8.55 (t, $J = 13.2$ Hz, 1H), 8.43-8.36 (m, 2H), 8.02-8.00 (m, 1H), 7.95-7.92 (m, 1H), 7.88-7.77 (m, 2H), 7.63-7.57 (m, 2H), 7.51-7.48 (m, 1H), 7.43-7.37 (m, 5H), 7.27 (t, $J = 5.4$ Hz, 1H), 7.09 (t, $J = 6.0$ Hz, 1H), 6.98 (s, 2H), 6.71 (s, 1H), 6.61 (s, 1H), 3.12-2.94 (m, 6H), 2.36 (s, 3H), 2.33-2.18 (m, 6H), 2.15 (s, 6H), 1.49 (s, 3H), 1.46 (s, 3H), 0.28-0.22 (m, 18H). HRMS (ESI): $[M]^+$, $C_{68}H_{67}BF_2N_2OS$ calculated: 1008.5035; found: 1008.5076. Compound **8d**: 1H -NMR (600 MHz, $CDCl_3$, ppm): δ 8.45-8.39 (m, 3H), 7.88-7.78 (m, 4H), 7.63-7.59 (m, 4H), 7.51-7.49 (m, 1H), 7.44-7.35 (m, 8H), 7.27 (s, 2H), 7.08 (s, 2H), 6.99 (s, 4H), 6.72 (s, 2H), 6.61 (s, 2H), 3.11-3.02 (m, 6H), 2.37 (s, 6H), 2.31-2.19 (m, 6H), 2.16 (s, 12H), 1.49 (s, 6H), 1.47 (s, 6H), 0.30-0.23 (m, 18H). HRMS (ESI): $[M]^+$, $C_{95}H_{92}B_2F_4N_4S_2$ calculated: 1450.6886; found: 1450.7007.

Acknowledgments

Support was provided by the CNRS (UMR 6302), the “*Université Bourgogne Franche-Comté*”, the “*Conseil Régional de Bourgogne*” through the PARI II CDEA project (Number: 2015-9205AAQ033S04150) and the European Regional Development Fund (FEDER-FSE Bourgogne 2014/2020). Convention n°2016-6200FE003S00257 (IGDA). Support was provided by National Key R&D Program of China (2016YFD0600804), National Natural Scientific Foundation of China (No. 21301092), Natural Scientific Foundation of Jiangsu Province, P. R. China

(No. BK20151513). JY is really thankful to the French Ministry of Research (MENSUR) for a PhD grant.

Appendix A. Supplementary data

Supplementary data related to this article can be found at <http://xxxxxxxxxxxxxx>.

References

- [1] Bodio E, Goze C. Investigation of B-F substitution on BODIPY and aza-BODIPY dyes: Development of B-O and B-C BODIPYs. *Dyes Pigments* 2019;160:700-10.
- [2] Boodts S, Fron E, Hofkens J, Dehaen W. The BOPHY fluorophore with double boron chelation: Synthesis and spectroscopy. *Coord Chem Rev* 2018;371:1-10.
- [3] Lu H, Mack J, Yang Y, Shen Z. Structural modification strategies for the rational design of red/NIR region BODIPYs. *Chem Soc Rev* 2014;43:4778–823.
- [4] Jean-Gérard L, Vasseur W, Scherninski F, Andrioletti B. Recent advances in the synthesis of [a]-benzo-fused BODIPY fluorophores. *Chem Commun.* 2018;54:12914-29.
- [5] Zhao J, Xu K, Yang W, Wang Z, Zhong F. The triplet excited state of Bodipy: formation, modulation and application. *Chem Soc Rev* 2015;44:8904–39.
- [6] Klifout H, Stewart A, Elkhalfi M, He H. BODIPYs for Dye-Sensitized Solar Cells. *ACS Appl Mater Interfaces* 2017;9(46):39873-89.
- [7] Thumuganti G, Gupta V, Singh SP. New dithienosilole- and dithienogermole-based BODIPY for solar cell applications. *New J Chem.* 2019;43:8735-40.
- [8] Wang X, Sun Q, Zhao L, Gong S, Xu L. Visualization of hydrogen polysulfides in living cells and in vivo via a near-infrared fluorescent probe. *J Biol Inorg Chem*

2019;24(7):1077-85.

- [9] Zhu X-Y, Wu H, Guo X-F, Wang H. Novel BODIPY-based fluorescent probes with large Stokes shift for imaging hydrogen sulfide. *Dyes and Pigments* 2019;165:400–7.
- [10] Ke X-S, Kim T, Lynch VM, Kim D, Sessler JL. Flattened Calixarene-like Cyclic BODIPY Array: A New Photosynthetic Antenna Model. *J Am Chem Soc* 2017;139(39):13950-6.
- [11] Turksoy A, Yildiz D, Akkaya EU. Photosensitization and controlled photosensitization with BODIPY dyes. *Coord Chem Rev.* 2019;379:47–64.
- [12] Turan IS, Gunaydin G, Ayan S, Akkaya EU. Molecular demultiplexer as a terminator automaton. *Nat Commun.* 2018;9:1-8.
- [13] Kolemena S, Akkaya EU. Chromogenic and Fluorogenic Sensing of Biological Thiols in Aqueous Solutions Using BODIPY-Based Reagents. *Coord Chem Rev.* 2018;354:121–34.
- [14] Zheng Q, Xu G, Prasad PN. Conformationally Restricted Dipyrromethene Boron Difluoride (BODIPY) Dyes: Highly Fluorescent, Multicolored Probes for Cellular Imaging. *Chem Eur J* 2008;14:5812–9.
- [15] Azarias C, Russo R, Cupellini L, Mennucci B, Jacquemin D. Modeling excitation energy transfer in multi-BODIPY architectures. *Phys Chem Chem Phys.* 2017;19(19):6443-53.
- [16] Yang J, Cai F-J, Yuan X-M, Meng T, Xin G-X, Wang S-F, et al. Efficient energy transfer in a tri-chromophoric dyad containing BODIPYs and corrole based on a

- truxene platform. *Journal of Porphyrins and Phthalocyanines*. 2018;22:777-83.
- [17] Maity A, Ghosh U, Giri D, Mukherjee D, Maiti TK, Patra SL. A water-soluble BODIPY based 'OFF/ON' fluorescent probe for the detection of Cd²⁺ ions with high selectivity and sensitivity. *Dalton Trans*. 2019;48:2108–17.
- [18] Maity A, Sil A, Nad S, Patra SK. A highly selective, sensitive and reusable BODIPY based 'OFF/ON' fluorescence chemosensor for the detection of Hg²⁺ Ions. *Sensors and Actuators B* 2018;255(1):299–308.
- [19] Wang S, Liu H, Mack J, Tian J, Zou B, Lu H, et al. A BODIPY-based 'turn-on' fluorescent probe for hypoxic cell imaging. *Chem Commun* 2015;51:13389–92.
- [20] Yang J, Fan Y, Cai F, Xu X, Fu B, Wang S, et al. BODIPY derivatives bearing borneol moieties: Enhancing cell membrane permeability for living cell imaging. *Dyes and Pigments*. 2019;164:105-11.
- [21] Küçüköz B, Sevinç G, Yildiz E, Karatay A, Zhong F, Yılmaz H, et al. Enhancement of two photon absorption properties and intersystem crossing by charge transfer in pentaaryl boron-dipyrromethene (BODIPY) derivatives. *Phys Chem Chem Phys*. 2016;18:13546-53.
- [22] Sui B, Bondar MV, Anderson D, Rivera-Jacquez HJ, Masunov AE, Belfield KD. New Two-Photon Absorbing BODIPY-Based Fluorescent Probe: Linear Photophysics, Stimulated Emission, and Ultrafast Spectroscopy. *J Phys Chem C* 2016;120(26):14317-29.
- [23] Zhang X, Xiao Y, Qi J, Qu J, Kim B, Yue X, et al. Long-Wavelength, Photostable, Two-Photon Excitable BODIPY Fluorophores Readily Modifiable for Molecular

- Probes. *J Org Chem* 2013;78(18):9153-60.
- [24] Yang J, Rousselin Y, Bucher L, Desbois N, Bolze F, Xu H-J, et al. Two-photon absorption properties of BODIPYs: units number from 1 to 4 versus geometry. *ChemPlusChem*. 2018;83(9):838-44.
- [25] Zhou Y, Cheung Y-K, Ma C, Zhao S, Gao D, Lo P-C, et al. Endoplasmic Reticulum-Localized Two-Photon-Absorbing Boron Dipyrromethenes as Advanced Photosensitizers for Photodynamic Therapy. *J Med Chem* 2018;61(9):3952–61.
- [26] Yılmaz H, Küçüköz B, Sevinç G, Tekin S, Yaglioglu HG, Hayval M, et al. The effect of charge transfer on the ultrafast and two-photon absorption properties of newly synthesized boron-dipyrromethene compounds. *Dyes and Pigments* 2013;99(3):979-85.
- [27] Goubard F, Dumur F. Truxene: a promising scaffold for future materials. *RSC Adv*. 2015;5:3521-51.
- [28] Shi K, Wang J-Y, Pei J. π -Conjugated Aromatics Based on Truxene: Synthesis, Self - Assembly, and Applications. *Chem Rec* 2015;15:52 – 72.
- [29] Cao X-Y, Zhang W-B, Wang J-L, Zhou X-H, Lu H, Pei J. Extended π -Conjugated Dendrimers Based on Truxene. *J Am Chem Soc* 2003;125(41):12430–1.
- [30] Miu L, Yan S, Yao H, Chen Q, Zhang J, Wang Z, et al. Insight into the positional effect of bulky rigid substituents in organic sensitizers on the performance of dye-sensitized solar cells. *Dyes and Pigments* 2019;168:1-11.
- [31] Tang D, Wan J, Xu X, Lee YW, Woo HY, Feng K, et al. Naphthobistriazole-based

- wide bandgap donor polymers for efficient non-fullerene organic solar cells: Significant fine-tuning absorption and energy level by backbone fluorination. *Nano Energy* 2018;53:258–69.
- [32] Wang B, Zeng Q, Sun Z, Xue S, Liang M. Molecularly engineering of truxene-based dopant-free hole-transporting materials for efficient inverted planar perovskite solar cells. *Dyes and Pigments* 2019;165:81-9.
- [33] Sharma R, Volyniuk D, Popli C, Bezikonny O, Grazulevicius JV, Misra R. Strategy Toward Tuning Emission of Star-Shaped Tetraphenylethene-Substituted Truxenes for Sky-Blue and Greenish-White Organic Light-Emitting Diodes. *J Phys Chem C* 2018;122:15614–24.
- [34] Yao C, Yu Y, Yang X, Zhang H, Huang Z, Xu X, et al. Effective blocking of the molecular aggregation of novel truxene-based emitters with spirobifluorene and electron-donating moieties for furnishing highly efficient non-doped blue-emitting OLEDs. *J Mater Chem C*. 2015;3:5783-94.
- [35] Lin T-C, Tsai B-K, Huang T-Y, Chien W, Liu Y-Y, Li M-H, et al. Synthesis and two-photon absorption properties of truxene-cored chromophores with functionalized pyrazine units fused as the end-groups. *Dyes and Pigments* 2015;120:99-111.
- [36] Po C, Tao C-H, Li K-F, Chan CKM, Fu HL-K, Cheah K-W, et al. Design, luminescence and non-linear optical properties of truxene-containing alkynylplatinum(II) terpyridine complexes. *Inorg Chim Acta* 2019;488:214–8.
- [37] Vinayakumara DR, Kumar M, P. Sreekanth P, Philip R, Kumar S. Synthesis,

- characterization and nonlinear optical studies of novel blue-light emitting room temperature truxene discotic liquid crystals. *RSC Adv.* . 2015;5(34):26596-603.
- [38] Yuan M-S, Wang Q, Wang W, Wang D-E, Wang J, Wang J. Truxene-cored π -expanded triarylborane dyes as single- and two-photon fluorescent probes for fluoride. *Analyst.* 2014;139:1541–9.
- [39] Zhu Y, Wang Z, Yang J, Xu X, Wang S, Cai Z, et al. N,N-Bis(2-pyridylmethyl)amine-Based Truxene Derivative as a Highly Sensitive Fluorescence Sensor for Cu^{2+} and Ni^{2+} Ion. *Chin J Org Chem* 2019;39(2):427-33.
- [40] Xu H-J, Bonnot A, Karsenti P-L, Langlois A, Abdelhammed M, Barbe J-M, et al. Antenna Effect in Truxene-bridged BODIPY-Triarylzinc(II)porphyrin Dyads: Evidence for a Dual Dexter-Förster Mechanism. *Dalton Trans.* 2014;43:8219-29.
- [41] Xie Y, Zhang X, Xiao Y, Zhang Y, Zhou F, Qi J, et al. Fusing three perylenebisimide branches and a truxene core into a star-shaped chromophore with strong two-photon excited fluorescence and high photostability. *Chem Commun* 2012;48:4338–40.
- [42] Tao J, Sun D, Sun L, Li Z, Fu B, Liu J, et al. Tuning the photo-physical properties of BODIPY dyes: Effects of 1, 3, 5, 7- substitution on their optical and electrochemical behaviours. *Dyes & Pigments* 2019;168:166–74.
- [43] Wang S, Lu H, Wu Y, Xiao X, Li Z, Kira M, et al. Silyl - and Disilanyl - BODIPYs: Synthesis via Catalytic Dehalosilylation and Spectroscopic Properties. *Chem Asian J.* 2017;12:561-7.
- [44] Yang J, Cai F, Desbois N, Huang L, Gros CP, Bolze F, et al. Synthesis,

spectroscopic characterization, one and two-photon absorption properties and electrochemistry of pi-expanded BODIPYs dyes *Dyes and Pigments*. 2020:submitted.

- [45] Nicoud J-F, Bolze F, Sun X-H, Hayek A, Baldeck P. Boron-Containing Two-Photon-Absorbing Chromophores. 3. One- and Two-Photon Photophysical Properties of p-Carborane-Containing Fluorescent Bioprobes. *Inorg Chem* 2011;50(10):4272–8.
- [46] Makarov NS, Drobizhev M, Rebane A. Two-photon absorption standards in the 550–1600 nm excitation wavelength range. *Optics Express*. 2008;16(6):4029-47.
- [47] Xu C, Webb WW. Measurement of two-photon excitation cross sections of molecular fluorophores with data from 690 to 1050 nm. *J Opt Soc Am B*. 1996;13:481-91.
- [48] Yuan M-S, Liu Z-Q, Fang Q. Donor-and-Acceptor Substituted Truxenes as Multifunctional Fluorescent Probes *J Org Chem* 2007;72:7915-22.

Graphical Abstract:

Synthesis, spectroscopic characterization, one and two-photon absorption properties and electrochemistry of truxene π -expanded BODIPYs dyes

Jian Yang, Hao Jiang, Nicolas Desbois, Guoliang Zhu, Claude P. Gros, Yuanyuan Fang, Frédéric Bolze, Shifa Wang, Hai-Jun Xu

Mono- and bis-BODIPY substituted truxene dyes exhibit remarkable two-photon absorption cross section σ_2 up to 6000 GM at 800 nm

